

DEUTSCHES ELEKTRONEN-SYNCHROTRON **DESY**

DESY 82-072
November 1982

CORRELATIONS IN ELECTRON-POSITRON,
LEPTON-HADRON AND HADRON-HADRON COLLISIONS

by

Wolfgang Koch

NOTKESTRASSE 85 · 2 HAMBURG 52

DESY behält sich alle Rechte für den Fall der Schutzrechtserteilung und für die wirtschaftliche Verwertung der in diesem Bericht enthaltenen Informationen vor.

DESY reserves all rights for commercial use of information included in this report, especially in case of filing application for or grant of patents.

**To be sure that your preprints are promptly included in the
HIGH ENERGY PHYSICS INDEX ,
send them to the following address (if possible by air mail) :**

**DESY
Bibliothek
Notkestrasse 85
2 Hamburg 52
Germany**

CORRELATIONS IN ELECTRON-POSITRON, LEPTON-HADRON AND HADRON-HADRON COLLISIONS *

Wolfgang Koch

Deutsches Elektronensynchrotron DESY, Hamburg

ABSTRACT

Recent results on two-particle correlations in rapidity space, forward-backward multiplicity correlations, charge correlations, flavour and baryon number correlations as well as Bose-Einstein correlations of identical particles are reviewed. Particular emphasis is given to the data from e^+e^- annihilation which serve in many respects as reference point in the interpretation of correlation phenomena observed in hadronic reactions.

Introduction

Correlations are basically a mathematical concept, not a physical one. This fact by itself implies the danger of a certain inhomogeneity in the physics subjects to be covered in such a presentation. Since correlations between physical observables play a role almost everywhere in particle physics and in particular in jet physics, the subject of my talk, if interpreted without any further restriction, would comprise an almost infinite field. Fortunately not all possible correlations between physical observables have been studied, which already facilitates my task substantially. However even among those topics that have been studied I will have to make a selection.

Extensive studies of correlations in multiparticle production by hadronic interactions started around 1975, mainly in the second generation experiments at the CERN Intersecting Storage Rings (ISR). An important result of the first studies was the existence of particle clusters in rapidity space. By 1979 very impressive material on various types of correlations was available, e.g. data on charge correlations, on correlations in transverse momentum and multiplicities. Subsequently, as physics interest at the ISR became focussed on high p_t interactions, correlation studies established the existence of four jets in this event class. Furthermore, correlations between the flavour content of the leading particle in the so-called trigger jet and the rapidity and

* Invited paper presented at the XIII International Symposium on Multiparticle Dynamics, Volendam, the Netherlands, 6-11 June 1982

charge distribution of the opposite jet give indications that a considerable fraction of high p_t jets might be due to hard gluon scattering.

These facts underline the importance of correlation studies in the effort to disentangle the complex production mechanism in hadronic reactions.

Whereas correlation studies in hadronic interactions have already a relatively long history, similar studies in e^+e^- annihilation were performed only in very recent time. For instance a first investigation of charge correlations in e^+e^- annihilation was published only in early 1981. It yielded direct evidence of the charged nature of the primary partons produced in this reaction. In contrast to hadronic interactions which contain 5 or 6 valence quarks already in the initial state, the final state in e^+e^- annihilation represents at parton level a relatively simple dynamical system: only one quark-antiquark pair, plus possibly a hard gluon, that arise from the decay of a massive photon. Therefore jets produced in e^+e^- annihilation have to be considered as the "cleanest" ones. The comparison of their properties, in particular that of their correlation behaviour to corresponding observations in interactions between hadrons is of extreme interest and, as will become evident, may serve as an important tool in the analysis of the much more complex production mechanism in hadronic interactions. For this reason, and also because I am working in the e^+e^- field, I will emphasize the correlation data from e^+e^- annihilation, which became available only very recently and are mostly unpublished. Unfortunately very few correlation data from hadrons produced in lepton-nucleon scattering are available at present.

In chapter I two-particle correlations will be discussed as measured in pp and $p\bar{p}$ interactions at the ISR and in e^+e^- annihilation at PETRA. The comparison of the short range correlation strengths will yield evidence for the assumption of two- (or more-) chain particle production in hadronic interactions.

Forward-backward multiplicity correlations are the subject of chapter II. Whereas substantial positive forward-backward multiplicity correlations were observed in hadronic interactions at high energies, in particular at the CERN $p\bar{p}$ collider, no genuine correlations of that type are found in e^+e^- annihilation.

In chapter III charge correlation studies in e^+e^- annihilation are presented. The short range correlation behaviour agrees with that observed in hadronic interactions. The long range charge correlations present direct evidence for the charge properties of the primary partons produced.

Chapter IV covers the scarce data on correlations within jets of quantum numbers other than charge.

Finally in chapter V we consider the Bose-Einstein correlation effect between identical particles. The almost complete saturation of this effect as observed recently in the process $e^+e^- \rightarrow J/\psi \rightarrow \text{hadrons}$, is compared to e^+e^- annihilation data at higher energies and to corresponding studies performed in hadronic interactions.

Correlations observed in high p_t physics at the ISR will not be subject of this presentation. They are reported in papers contributed to this conference by A. Putzer and K. Rauschnabel. Likewise the energy weighted angular correlations in e^+e^- annihilation, which have been given much attention at recent conferences as a special method to determine the strong coupling constant α_s , will have to be omitted. The results of the CELLO Collaboration on this subject have been presented to this conference by C. Kiesling.

I. Two-Particle Correlations in Rapidity Space

Before discussing recent results from $pp/p\bar{p}$ collisions and e^+e^- annihilations, we need a few words about definitions and conventions. The rapidity y is defined as usual to be $y = 1/2 \ln [(E + p_{||}) / (E - p_{||})]$ where in hadronic reactions $p_{||}$ is defined with respect to the incident beam direction and in e^+e^- annihilation with respect to the sphericity axis.

The two-particle correlation function¹⁾

$$C^{ab}(y,y') = \rho_2^{ab}(y,y') - f \rho^a(y)\rho^b(y') \quad (\text{I.1})$$

compares the two-particle density $\rho_2^{ab}(y,y') = (1/\sigma_{\text{inel}}) d\sigma^{ab}/dydy'$ to its statistically uncorrelated expectation value which is the product of single particle densities $\rho^a(y)$ and $\rho^b(y')$ at y and y' , respectively.

The indices a and b denote particle properties, e.g. charge. The factor f in eq.(I.1) is a matter of convention. Whereas several authors set $f \equiv 1$ others employ the definition

$$f = \langle n^a n^b - \delta^{ab} \rangle / (\langle n^a \rangle \langle n^b \rangle) \quad (\text{I.2})$$

where n^a, n^b are particle multiplicities and $\langle \rangle$ denotes the average over the event sample. The quantity δ^{ab} is equal to 0 for different particle labels, a, b and equal to 1 for identical or undistinguished labels. Convention (I.2) ensures that $C(y,y') \equiv 0$ for events with particles uncorrelated in y . The normalized correlation function

$$R^{ab}(y,y') = \frac{C^{ab}(y,y')}{f \rho^a(y)\rho^b(y')} = \frac{\rho_2^{ab}(y,y')}{f \rho^a(y)\rho^b(y')} - 1 \quad (\text{I.3})$$

is more appropriate than $C^{ab}(y,y')$ for comparing the correlation behaviour

of reactions with different average multiplicities. Furthermore R is rather insensitive to acceptance corrections.

Let us first consider the results on particle correlations in pp and $p\bar{p}$ collisions obtained by the ABCHW Collaboration²⁾ with the Split Field Magnet (SFM) detector at the ISR, at $\sqrt{s} = 53$ GeV CM energy. Displayed in Fig. 1a) to d) is the normalized correlation function $R(y,y')$ with $f = 1$ for fixed values of $y' = -1, 0, 1, 2$. Events with at least 8 charged tracks ($N_{tr} \geq 8$) were used and all charged particles were assumed to be pions. R shows the same behaviour for pp (closed circles) and $p\bar{p}$ collisions (open circles). It is characterized by the well known local maxima at $y \sim y'$ indicative of the production of particle clusters.

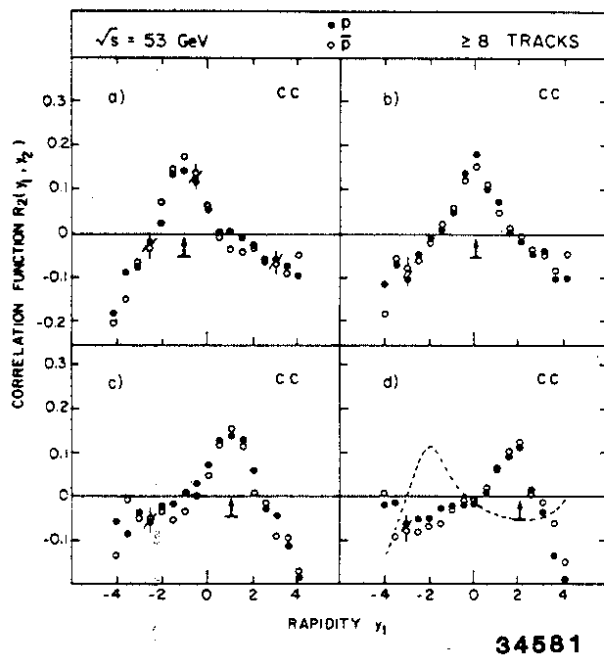


Fig.1 Correlation function $R_2(y_1, y_2)$ for all charge combinations (cc) of hadron pairs in $pp/p\bar{p}$ collisions at $\sqrt{s} = 53$ GeV. ABCHW Collaboration²⁾

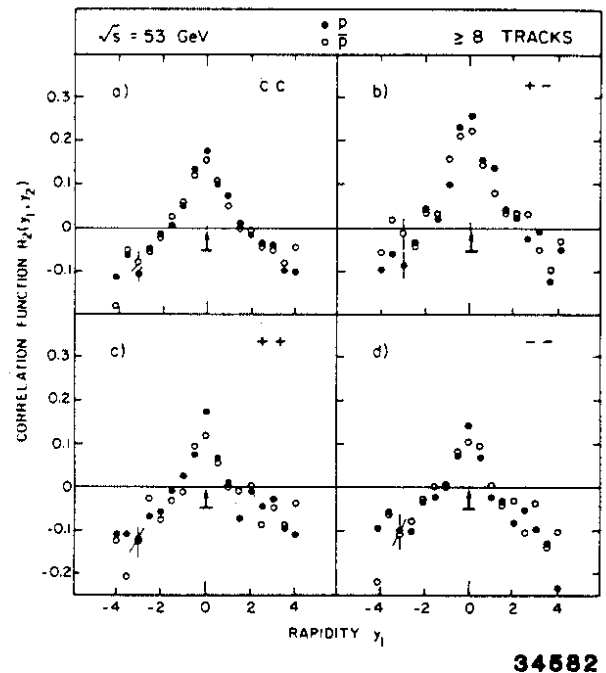


Fig.2 Correlation functions $R_2(y_1, y_2) = 0$ for cc, +- combinations of hadrons in $pp/p\bar{p}$ collisions at $\sqrt{s} = 53$ GeV. ABCHW Collaboration²⁾

Fig. 2 shows $R(y,y')$ for $y' = 0$, a) for the combination of any two charged particles labelled cc, b) for +- combinations, c) for ++ and d) for -- combinations. The peak in the correlation function at $y \sim y'$ is also present for equal charge combinations although less pronounced than in the case of opposite charges. Qualitatively this can be explained by the fact that on average more opposite charge pairs than equal charge pairs will arise from resonance decays.

We compare the pp and $p\bar{p}$ data with corresponding results from e^+e^- collisions at $\langle\sqrt{s}\rangle = 34$ GeV evaluated by the TASSO Collaboration from ~15 000 hadronic events observed at various CM energies between 27 and 35 GeV^{3,4)}.

Figs. 3a) to 3d) show $R(y,y')$ for different intervals of y' . The data include only events with ≥ 6 charged tracks produced, including K_S^0 decays. They are corrected for acceptance losses.

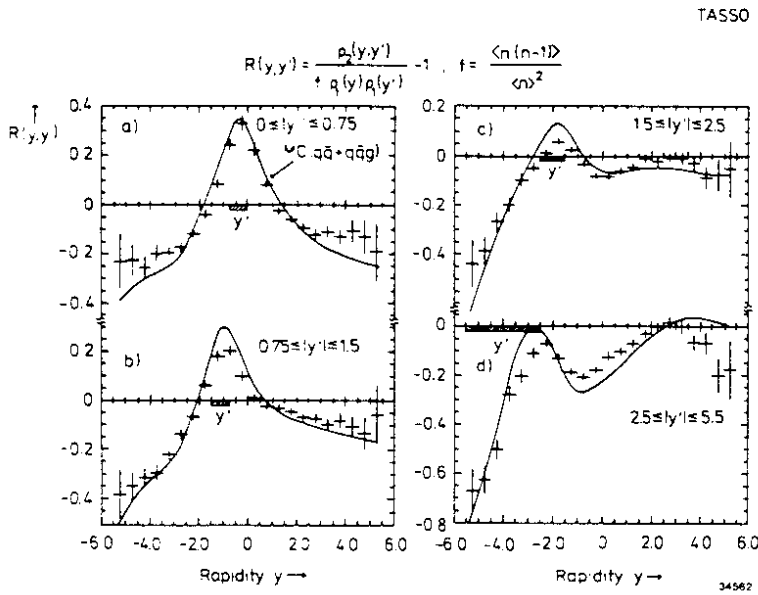


Fig.3 Correlation functions $R(y,y')$ for any charge combinations of hadrons in e^+e^- at $\sqrt{S} = 34$ GeV. TASSO Collaboration

remarkably good when taking into account that the free parameters of the model had been adjusted without using any correlation data at all⁷⁾.

Except for the outer y' interval (Fig. 4d) where energy momentum conservation suppresses the simultaneous production of neighbouring particles,

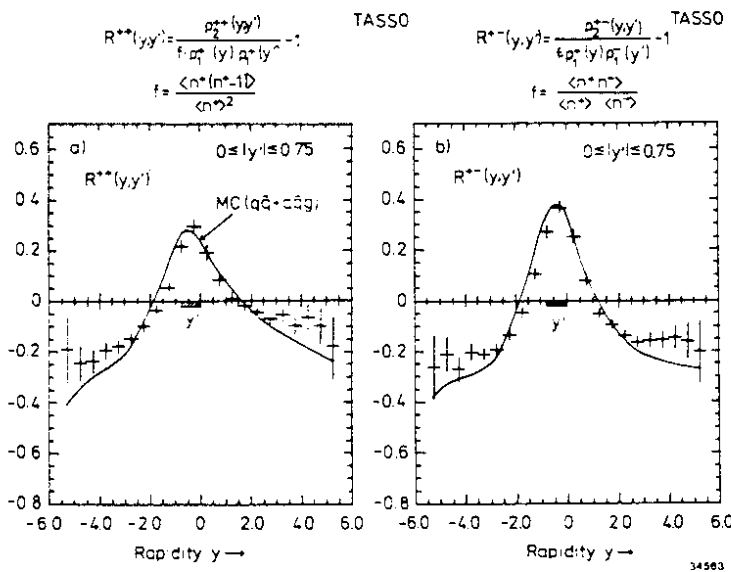


Fig.4 Correlation functions $R(y,y')$ at $y' \approx 0$ for a) ++ and b) +- combinations in e^+e^- at $\sqrt{S} = 34$ GeV. TASSO Collaboration

The rapidity is calculated with respect to the sphericity axis of the event assigning the pion mass to all charged particles. The curves in Fig. 3 represent the prediction of a Field-Feynman type⁵⁾ jet fragmentation Monte Carlo program⁶⁾ (Hoyer et al.), taking into account $q\bar{q}$ and $q\bar{q}g$ production in the appropriate proportion. The agreement of the data with the predictions of the fragmentation model, henceforth referred to as MC($q\bar{q} + q\bar{q}g$), is

e^+e^- data and fragmentation model exhibit peaks of the correlation function at values $y \sim y'$, similar to those in the data from hadron collisions. From the satisfactory agreement between the data and MC($q\bar{q} + q\bar{q}g$) we conclude that at least in $e^+e^- \rightarrow$ hadrons there is no need to invoke the existence of clusters other than the known resonances to explain the behaviour of $R(y,y')$. In

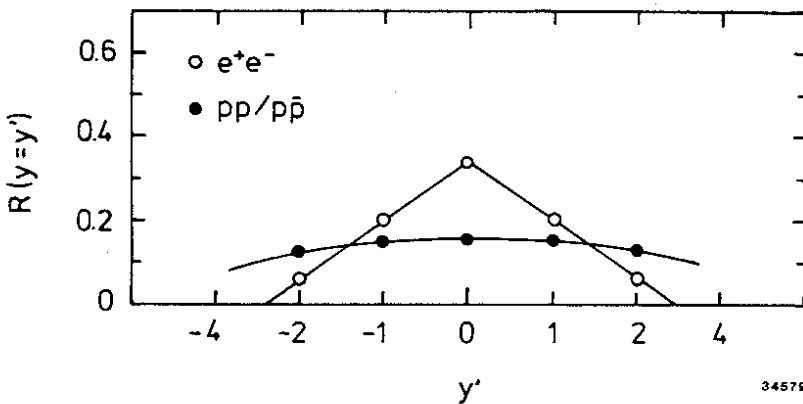
MC($q\bar{q} + q\bar{q}g$) the fraction of vector mesons produced was assumed to be 45 %, in agreement with recent measurements ⁸).

Fig. 4a) shows $R(y,y')$ for combinations of equal charges, Fig. 4b) for opposite charges, both evaluated for the central y' interval $|y'| \leq 0.75$. As in the case of pp and $p\bar{p}$ collisions (Fig. 2) $R^{+-}(y \approx y')$ is larger than $R^{++}(y \approx y')$. Again the prediction of MC($q\bar{q} + q\bar{q}g$) is shown as full line. It should be recalled that in the e^+e^- analysis the factor f in eq.(I.3) was determined from eq.(I.2), yielding $f^{CC} = 1.03$, $f^{++} = 0.96$, $f^{+-} = 1.11$, whereas in the $pp/p\bar{p}$ data f was set equal to 1.

Although qualitatively very similar, the correlation functions measured in $pp/p\bar{p}$ and in e^+e^- collisions show definite quantitative differences, which are visualized in Table 1 and Fig. 5. Here we compare the peak values $R(y = y')$ of the correlation functions measured in $pp/p\bar{p}$ and e^+e^- .

Table 1. Comparison between $R(y,y')$ from e^+e^- and from $pp/p\bar{p}$ collisions.

	SFM : $p\bar{p}/pp$	TASSO : e^+e^-
\sqrt{S}	53 GeV	34 GeV
y_{\max}	5.9	5.5
FWHM of $d\sigma/dy$	6.0	4.8
charged tracks N_{tr}	≥ 8	≥ 6
$R(y = y'), y = 0$	0.15	0.34
$y = 1$	0.15	0.20
$y = 2$	0.125	0.06



From Fig. 5 we conclude that $R(0, 0)$ as observed in e^+e^- is about 2 times as large as that in $pp/p\bar{p}$ collisions and that with increasing $|y|$ the peak values $R(y = y')$ drop faster in e^+e^- than in hadronic collisions.

Fig.5 Height of local maxima of correlation function $R^{CC}(y,y')$ at $y \approx y'$ for e^+e^- at $\sqrt{S} = 34$ GeV and $p\bar{p}$ collisions at $\sqrt{S} = 53$ GeV.

Both observations find a rather straightforward explanation

if one assumes that in $pp/p\bar{p}$ interactions particles are produced in two

(or more) overlapping chains (strings) in contrast to $e^+e^- \rightarrow q\bar{q}$ where only one such chain is present. This idea is for instance expressed in the multichain dual parton model based on dual topological unitarization⁹⁾. According to this model final state hadrons are produced in chains linking either a quark to an antiquark as in $e^+e^- \rightarrow q\bar{q}$ or a quark to a diquark as in deep inelastic lepton-nucleon scattering. Hadron production in pp collisions would then proceed to lowest order via two colour-neutral quark-diquark chains as sketched in Fig. 6.

It is easy to show that the superposition of two independent chains with correlation functions $R^{(1)}$ and $R^{(2)}$, respectively, yields as resulting correlation function for $y = y'$

$$R^{\text{res}} = \left[R^{(1)} \rho_1^{(1)2} + R^{(2)} \rho_1^{(2)2} \right] / \left[\rho_1^{(1)} + \rho_1^{(2)} \right]^2 \quad (\text{I.4})$$

If chains 1 and 2 have the same densities then $R^{\text{res}} = (1/2)R^{(1)} = (1/2)R^{(2)}$, i.e. the resulting correlation function is reduced to half the single chain value. Consequently, if one assumes that the single $q\bar{q}$ chain in e^+e^- annihilation has approximately the same correlation function R as one of the $q - q\bar{q}$ chains in pp collisions then the difference between $R(y = y' = 0)$ from e^+e^- and that from pp/pp̄ (Fig. 5) is almost quantitatively explained.

It has to be mentioned that the pp/pp̄ data sample with $N_{\text{tr}} \geq 4$ (not shown here) yields an $R(y = y' = 0)$ value rather close to that observed in e^+e^- annihilation. However this sample contains the class of single and double diffraction dissociation events, which, due to their special production mechanism, cannot be compared to those from e^+e^- annihilation. These events have $\rho_1(y = 0) = 0$, $\rho_2(y = y' = 0) = 0$. A 13 % contribution of diffraction events in the $N_{\text{tr}} \geq 4$ sample would explain the observed difference in $R(0,0)$ between this and the $N_{\text{tr}} \geq 8$ sample. Such a yield of diffraction events does not appear unreasonably high.¹⁾

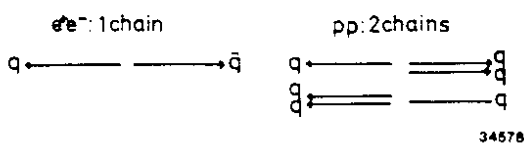


Fig.6 Chain production in e^+e^- and pp collisions.

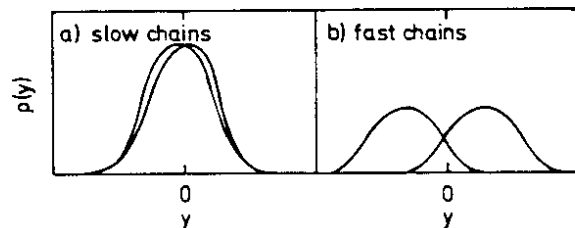


Fig.7 Rapidity distribution in different chain configurations.

The fact that $R(y,y')$ drops with increasing $|y|$ much more slowly in the pp/pp̄ case than in e^+e^- can be explained by the kinematics of the two-chain

production. Let us assume, for the sake of simplicity, that the two chains are produced in only two kinematical configurations as depicted in Fig. 7. In case 1 the centres of gravity of the two chains are at rest in the CM and give rise to fully overlapping particle density distributions, as shown in Fig. 7a). In case 2 (Fig. 7b) the chains have smaller rest mass and move rapidly in the common CM. Particle pairs produced at $y = y' = 0$ will predominantly arise from case 1 in which, due to the full overlap, the value of $R(y = y' = 0)$ will be reduced by a factor of ~ 2 with respect to the case of one chain only as in e^+e^- . On the other hand, particle pairs produced at e.g. $y = 2$ will arise from both cases considered in comparable proportion. Case 1 will contribute a very small R while case 2 will contribute the high R measured in the centre of the single chain. The superposition of the two kinematical configurations will yield an average R at e.g. $y = y' = 2$ close to that observed at $y = y' = 0$. In this way the comparatively flat behaviour of $R(y,y')$ in hadronic collisions can be qualitatively understood.

In summary, if one assumes a similar correlation behaviour of $q - \bar{q}$ and $q - qq$ chains the comparison of the correlation functions $R(y,y')$ observed in hadronic collisions and e^+e^- annihilation yields probably the strongest experimental evidence presently known for multiparticle production by two (or more) largely uncorrelated chains in hadronic collisions. In this context it has to be emphasized that data on short range correlations from high energy lepton-nucleon scattering (single $q - qq$ chain) would be very desirable.

Conclusions on two-particle correlations:

- Two-particle correlations in pp and $p\bar{p}$ collisions at $\sqrt{s} = 53$ GeV are the same within errors, thus reflecting a similar production mechanism.
- The two-particle correlation behaviour in e^+e^- annihilation is satisfactorily described by the Field-Feynman jet fragmentation model. In particular it appears unnecessary to invoke production of particle clusters other than the known resonances.
- The maximum of the normalized correlation function $R(y,y')$ at $y = y' = 0$ is about twice as high in e^+e^- annihilations as in $pp/p\bar{p}$ inelastic collisions. With increasing $|y|$ the local maximum of R at $y = y'$ decreases much faster for e^+e^- than for $pp/p\bar{p}$. These observations can be consistently explained by assuming particle production in a single $q - \bar{q}$ chain for the case of e^+e^- annihilation, and production in two largely uncorrelated $q - qq$ chains (plus possibly more chains at higher energies) for hadronic inelastic

interactions, where the $q - q\bar{q}$ chains are assumed to have a similar correlation behaviour as the $q - \bar{q}$ chains. The comparison of the correlation functions observed in e^+e^- annihilation and in hadronic inelastic events as shown in Fig. 5 yields indeed very strong experimental evidence for two- or multichain production in hadron interactions.

II. Forward-Backward Multiplicity Correlations

Not only short range particle correlations, as studied in the previous chapter, but also long range correlations between particles or groups of particles produced at larger distances in rapidity, may give valuable information about the multiparticle production mechanism.

We will consider the correlation between the multiplicity of particles emitted into one CM hemisphere, defined with respect to the direction of the projectile, and the multiplicity in the opposite hemisphere. This is called the forward-backward (F-B) multiplicity correlation. In Fig. 8 we present a compilation by A. Wróblewski¹⁰⁾ of pp data at various energies, showing the average

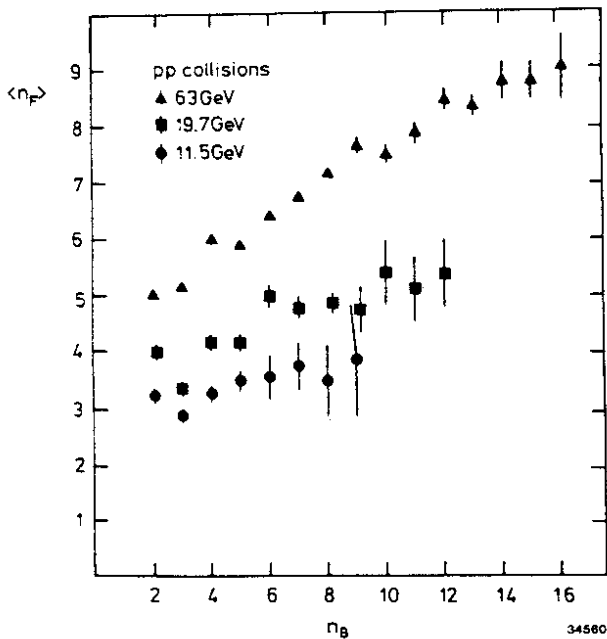


Fig.8 $\langle n_F \rangle$ as a function of n_B in pp collisions at different CM energies. Private communication by A. Wróblewski¹⁰⁾.

multiplicity in the forward hemisphere, $\langle n_F \rangle$, as a function of the discrete multiplicity in the backward hemisphere, n_B . The average forward multiplicity $\langle n_F \rangle$ exhibits an approximately linear rise as a function of n_B . The slope $d\langle n_F \rangle/dn_B$ is a measure of the correlation strength and clearly rises with energy. Fitting straight lines $\langle n_F \rangle = a + bn_B$ to these data, Wróblewski observes to good approximation a linear rise of the slope $b = d\langle n_F \rangle/dn_B$ with $\ln S$, the logarithm of the CM energy squared.

This is displayed in Fig. 9. Recent results from the UA5 experiment at the CERN $p\bar{p}$ collider demonstrate the continuation of this rise of the correlation strength to $\sqrt{S}=540$ GeV. Figs.10a,b) show $\langle n_F \rangle$ as a function of n_B as measured by the UA5 experiment¹¹⁾, where in Fig. 10a) only particles in the interval of pseudorapidity $|\eta| \leq 1$ are considered and in Fig. 10b) particles in the interval $1 \leq |\eta| \leq 4$, where pseudorapidity is defined as usual to be $\eta = -\ln \operatorname{tg} \frac{\theta}{2}$, θ being the particle

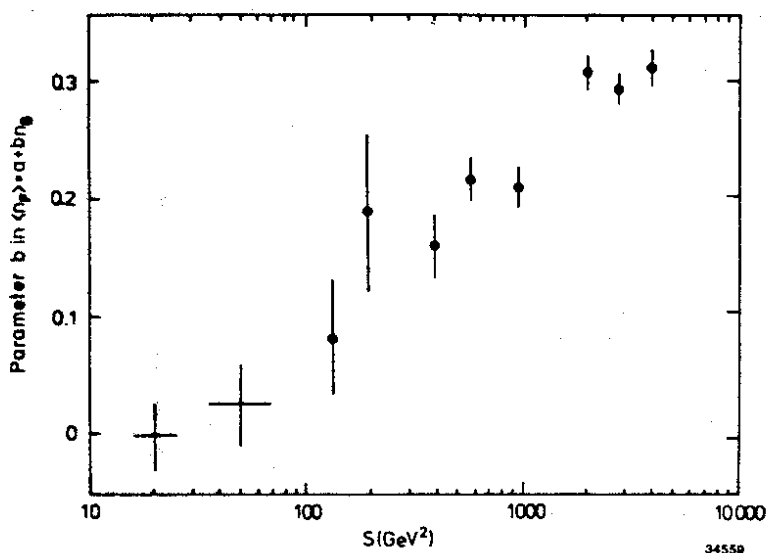


Fig.9 Slope parameter b in $\langle n_F \rangle = a + bn_B$ for pp collisions as a function of S . Private communication by A. Wróblewski¹⁰⁾.

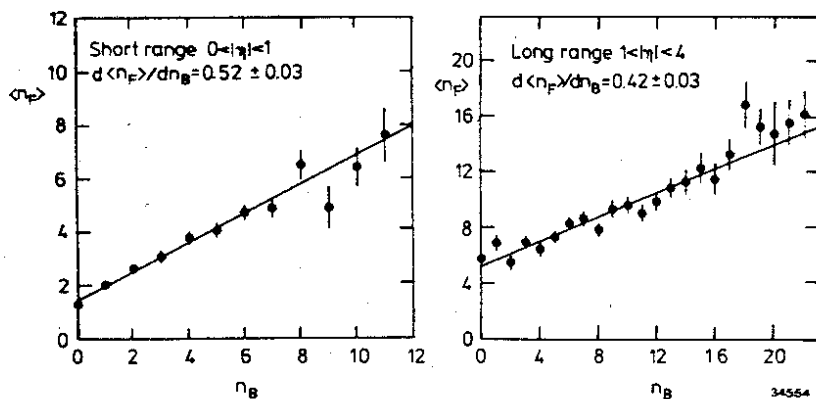


Fig.10 $\langle n_F \rangle$ as a function of n_B for short ($0 < |\eta| < 1$) and long ($1 \leq |\eta| \leq 4$) distances in pseudorapidity η , measured by the UA5 Collaboration in $p\bar{p}$ at 540 GeV.

emission angle in the CM with respect to the beam direction. Particles emitted into one hemisphere are separated from those emitted into the opposite one by at most 2 units of η in the case of Fig. 10a) and by at least 2 units of η in the case of Fig. 10b). Therefore the slopes $b = d \langle n_F \rangle / dn_B$ in Figs. 10a) and 10b) measure the strength of short-range and long-range multiplicity correlations, respectively. The values are $b = 0.52 \pm 0.03$ for the short range case and $b = 0.42 \pm 0.03$ for the long range case.

In Fig. 11 the strengths of short range and long range multiplicity correlations are compared as a function of S ¹¹⁾. The short range correlation strength is already substantial at low energies and increases only slightly with S . On the other hand the strength of long range

multiplicity correlations is negligible at low energies and reaches almost the strength of short range correlations at $p\bar{p}$ collider energies.

What does one expect for e^+e^- annihilation? There are essentially two classes of theoretical concepts describing the hadronization process. In perturbative (or probabilistic) models, like that of Field and Feynman⁵⁾, the hadronization of any given emitted parton proceeds essentially independently of that of another one. Such models predict rather small F-B multiplicity correlations in e^+e^- . The other class of models, sometimes quoted as non-perturbative, view hadronization as the explosion of a single colour flux tube. For example in the model of Kühn and Schneider¹²⁾ the first stage of this explo-

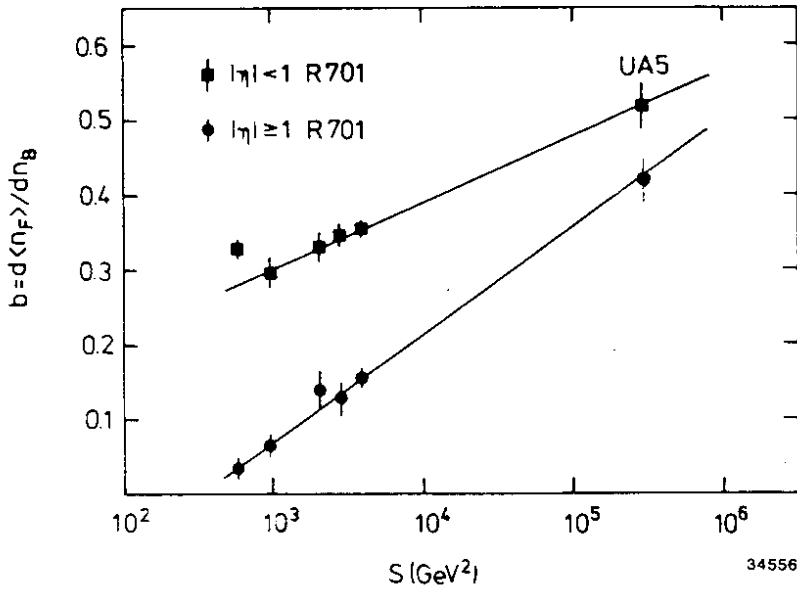


Fig.11 Strength $b = d \langle n_F \rangle / dn_B$ of short range ($|\eta| < 1$) and long range ($|\eta| > 1$) F-B multiplicity correlations as a function of S .

basic ingredients are the same as those used in similar models¹³⁾ describing F-B multiplicity correlations in pp collisions. The predictions of this model for the dependence $\langle n_F \rangle = f(n_B)$ is shown in Fig.12 where the curves correspond to various values of the average charged multiplicity \bar{n} . From Fig. 12 one calculates for e^+e^- at $\sqrt{S} = 34$ GeV, assuming $\bar{n} \approx 14$, a correlation strength $b = d\langle n_F \rangle / dn_B \approx 0.25$.

In Fig. 13 experimental results on the F-B multiplicity correlation in e^+e^- are plotted. The data, obtained by the TASSO collaboration at $\sqrt{S}=34$ GeV, include only events with an observed charged multiplicity $n_{ch}^{obs} > 5$ and are not corrected for losses induced by acceptance limitations of the apparatus. The full line in Fig. 13 is the prediction of the Feynman-Field type jet fragmentation model MC($q\bar{q} + q\bar{q}g$) already referred to in chapter I. In this model jets fragment completely independently of each other up to a final overall kinematical rearrangement that ensures energy-momentum conservation. The free parameters of the model have not been adjusted to any particle or multiplicity correlations. From the almost perfect agreement of the model with the data we have to conclude that long range multiplicity correlations as observed in pp collisions are absent in e^+e^- annihilation. A certain amount of long range multiplicity correlation of trivial nature is, however, also expected in e^+e^- due to the pair production of quarks of different flavour and their different fragmentation properties. Charm and bottom quarks will yield on average a larger multiplicity in both hemispheres than light quarks. In fact the rising

sion is characterized by the formation of energy clusters or fireballs which further cascade down. Large fluctuations of the field strength extending over the whole flux tube will influence the particle density in all regions of longitudinal phase space simultaneously, thus giving rise to strong long range multiplicity correlations. The model of Kühn and Schneider allows for such fluctuations and satisfies KNO scaling. Its

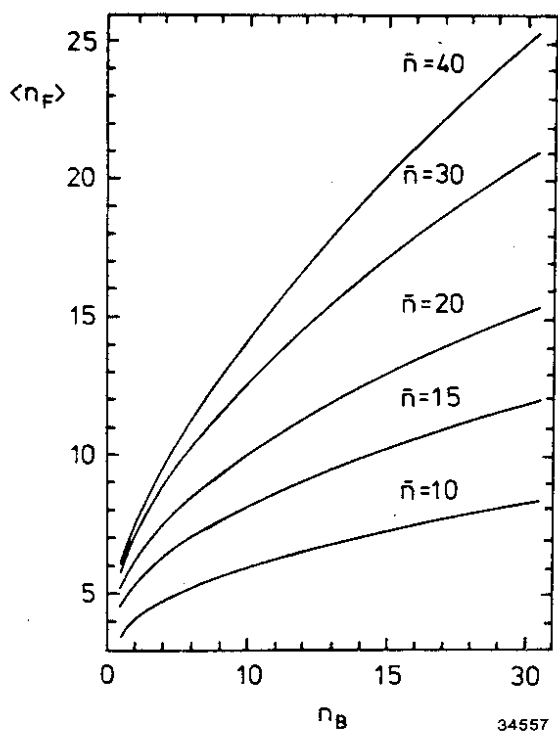


Fig.12 $\langle n_F \rangle$ as a function of n_B for different average multiplicities \bar{n} as predicted for e^+e^- annihilation by J.H. Kühn and H. Schneider¹²⁾.

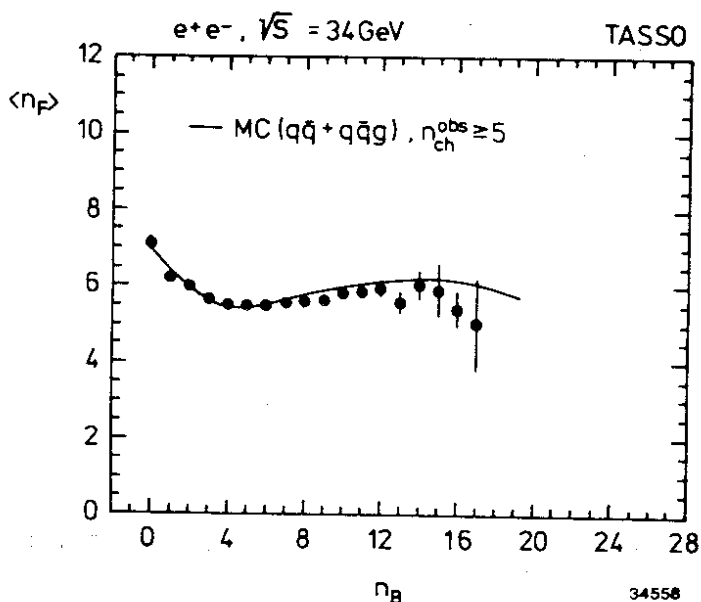


Fig.13 $\langle n_F \rangle$ as a function of n_B in e^+e^- at $\sqrt{S} = 34 \text{ GeV}$, for events with at least 5 observed charged tracks, uncorrected for acceptance losses. The curve is the prediction of the Field-Feynman jet fragmentation model. TASSO Collaboration³⁾

slope in the middle portion of the MC curve and the data in Fig. 13 can be mainly ascribed to this effect. Another contribution to the positive slope is due to remaining short range correlations, which have not been removed by cutting out a central rapidity interval as in the UA5 analysis. The negative slope at low values of n_B is due to the multiplicity cut $n_{ch}^{obs} \geq 5$.

To further elucidate the multiplicity correlation behaviour in e^+e^- we present in Fig. 14 Monte Carlo studies for the case of complete geometric acceptance. Curve a) corresponds to the curve in Fig. 13, thus reflecting the actual behaviour of the data when corrected for acceptance losses. The steepest local slope around $n_B = 7$ amounts to 0.18, rather close to the value of 0.25 predicted by the model of Kühn and Schneider¹²⁾. Curve b) in Fig. 14 represents the prediction for the case that only u and d quarks were produced. The slope is substantially smaller than that of curve a) showing that the major part of the correlation strength observed is due to quark production of different flavours. Curve c) is the same as curve b) (only u and d quark production) except that the multiplicity cut has been lowered from $n_{ch}^{prod} \geq 6$ to $n_{ch}^{prod} \geq 2$, which removes the negative slope at low values of n_B . For higher values of n_B curves b) and c) coincide. Finally in curve d) the

effects of short range correlations have been removed by complete suppression of vector meson production and by preventing K_S^0 from decaying. The remaining small but finite positive slope is due to the decay of heavier pseudoscalars like η and η' which, within the given Monte Carlo program, could not easily be prevented from being produced nor from decaying.

These Monte Carlo studies suggest that the non-vanishing long range multiplicity correlations observed in e^+e^- annihilations are entirely due to trivial effects: the production of different quark flavours and a remaining part of short range correlations induced by decays of resonances and of heavy pseudoscalars. These (trivial) effects are of completely different nature than those considered by Kühn and Schneider¹²⁾ or those acting in pp collisions at high energies.

In a contribution to this conference Fiałkowski and Kotański¹⁴⁾ have shown that the F-B multiplicity correlations observed at ISR energies can entirely be described as a kinematical effect due to internal degrees of freedom. If for instance 2 heavy chains are produced at rest in the CM system, more particles will be emitted into both hemispheres than in the case when two chains of low rest mass are moving rapidly into opposite directions. Averaging over all possible kinematical configurations of the two-chain process will introduce long range multiplicity correlations by the chain energy spread, even if in each single chain such correlations do not exist. In the model of Fiałowski and Kotański the weights for different kinematical configurations of two-chain production are determined by the quark momentum distribution inside the proton, as derived from the proton structure functions.

It was pointed out at this conference by A. Capella that the extremely strong F-B multiplicity correlations found at collider energies could not be explained by the kinematics of two-chain processes alone. At these energies more than two chains would have to contribute to understand the experimental results.

Finally we show in Fig. 15 F-B correlations, as observed in vp scattering between the current jet and the spectator jet¹⁵⁾. As in e^+e^- also here the hadronization is supposed to proceed via a one-chain process, here a $q - qq$ chain. The data are certainly compatible with the assumption of no genuine long range multiplicity correlations. The small effect possibly present could most likely be interpreted as a contribution from short range correlations.

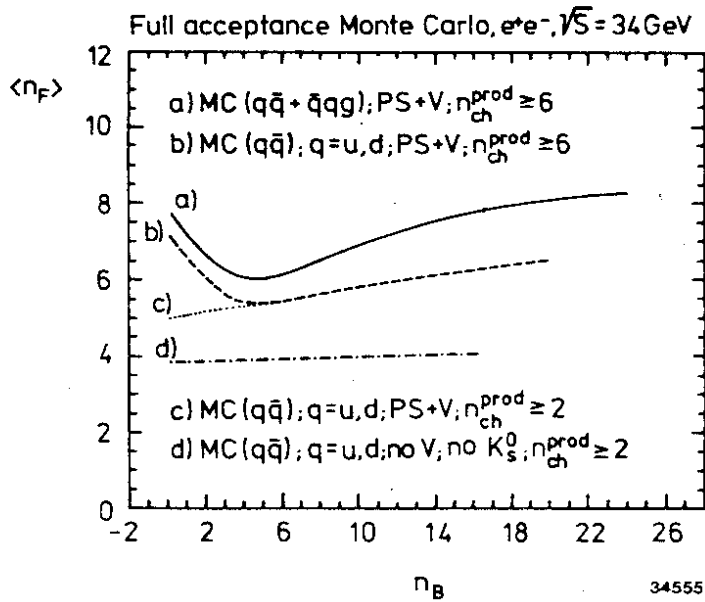


Fig.14 Monte Carlo studies of F-B multiplicity correlations in e^+e^- . See explanations in the text.

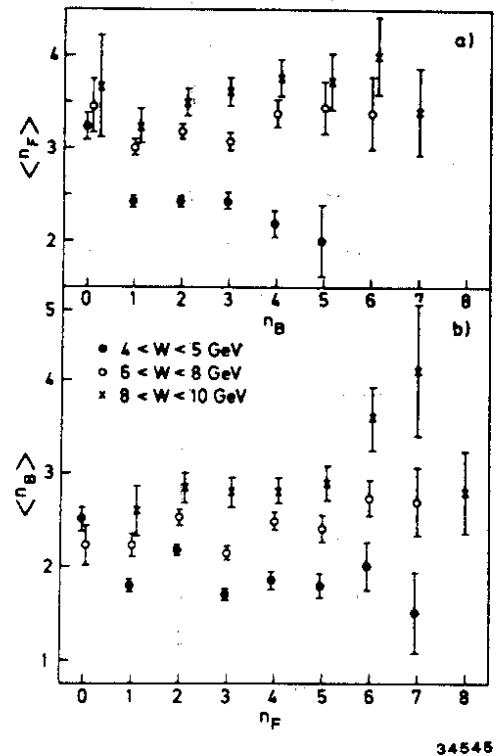


Fig.15 F-B multiplicity correlations for charged hadrons in νp scattering for three W intervals, from BEBC νH_2^{15}). F refers to the direction of the current jet.

Conclusions on F-B multiplicity correlations.

- F-B multiplicity correlations in hadronic reactions rise about linearly with $\ln S$.
- In e^+e^- annihilations no non-trivial long range F-B correlations are observed. The measured correlation behaviour may be explained as due to pair production of different quark flavours plus contributions from short range correlations.
- F-B correlations between hadrons produced in νp reactions are negligible within errors or reflect contributions from short range correlations only.
- The long range multiplicity correlations measured in hadronic reactions can be interpreted as kinematical effect due to internal degrees of freedom (chain energy spread) in the production of two or more particle chains, neither of which has to show long range multiplicity correlation in its own CM.

III. Charge Correlations in Rapidity Space

Charge correlations can be described in an appropriate and convenient way by introducing the concept of charge compensation. In an event with net charge zero the charge of the k 'th particle, e_k , is compensated, i.e. neutralized, by the sum of all other charges:

$$e_k = - \sum_{i \neq k}^n e_i \quad (III.1)$$

The charge compensation "probability" for a particle k produced at $y' = y_k$ in a particular event is given by the expression

$$p(y, y' = y_k) = \frac{1}{\Delta y} \sum_{i \neq k}^n (-e_k e_i) \delta_{iy} \quad (III.2)$$

where $(-e_k e_i)$ is +1 for opposite charges and -1 for equal charges e_i, e_k . The symbol δ_{iy} in eq.(III.2) is equal to +1 if particle i lies inside the interval Δy and zero otherwise. Note that $p(y, y' = y_k)$, although locally negative, is normalized to 1:

$$\int p(y, y' = y_k) dy = 1 \quad (III.3)$$

Generalizing eq.(III.2) we introduce a two-particle density $\phi(y, y')$ which we will call "compensating charge flow":

$$\begin{aligned} \phi(y, y') &= \frac{1}{\Delta y \Delta y'} \sum_{k=1}^n e_k \delta_{ky'} \left(\sum_{i \neq k}^n e_i \delta_{iy} \right) \quad (III.4) \\ &= \left[\rho_2^{+-}(y, y') + \rho_2^{-+}(y, y') \right] - \left[\rho_2^{++}(y, y') + \rho_2^{--}(y, y') \right] \end{aligned}$$

and a charge compensation probability

$$\tilde{\phi}(y, y') = \phi(y, y') / \int \phi(y, y') dy = \phi(y, y') / \rho(y') \quad (III.5)$$

Fig. 16 shows the charge compensation probability $\tilde{\phi}(y, y')$ for 4 different y' intervals of the reference particle, as measured in e^+e^- at $\sqrt{S} = 34$ GeV by the TASSO collaboration^{3,16}). The data are corrected for acceptance losses and refer to $n_{ch}^{prod} \geq 6$. We observe that charge compensation reaches relative maxima at $y \approx y'$, a clear short range effect. For the central interval $-0.75 \leq y' \leq 0$ (Fig. 16a) $\tilde{\phi}$ drops with y about symmetrically to both sides, becoming negligible at values ~ 2.5 units of rapidity apart from y' . However, when selecting reference particles at higher values of $|y'|$, ϕ exhibits a tail at opposite values of y , particularly well developed for the outer interval $y' < -2.5$ in Fig.16d. This long range effect in charge compensation is considered as direct evidence that the primary partons produced in e^+e^- annihilation are charged¹⁶.

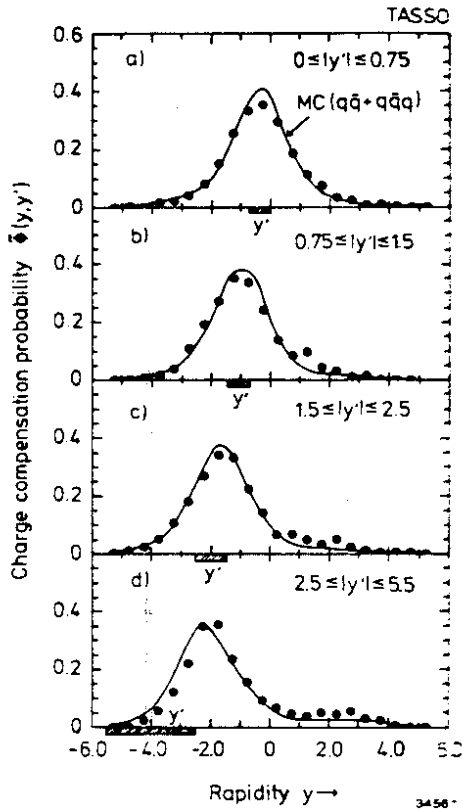


Fig.16 Charge compensation probability $\phi(y, y')$ [eq.(III.5)] as a function of rapidity y for particles produced at y' . Data from $e^+e^- \rightarrow$ hadrons at $\sqrt{s} = 34$ GeV, measured by TASSO Collaboration³⁾.

Short range charge compensation in e^+e^- due to resonance decays and to local charge compensation in the quark-gluon cascade is very similar to that observed in hadron collisions. This can be seen from Fig. 17 which shows the so-called "associated charge density balance" Δq as measured in pp collisions at $\sqrt{s} = 52$ GeV at the ISR¹⁷⁾. This quantity

$$\Delta q(y, y') = \frac{\rho^{-+}(y, y') - \rho^{++}(y, y')}{\rho^+(y')} + \frac{\rho^{+-}(y, y') - \rho^{--}(y, y')}{\rho^-(y')} \quad (\text{III.6})$$

would be (up to a factor of 2) identical to $\tilde{\phi}$ when applied to a system with net charge zero and local charge density identical to zero. In fact when choosing reference particles at $y' = 0$ the charge compensation lengths (FWHM) measured in e^+e^- and pp collisions are practically the same: 2.75 units of rapidity in e^+e^- ³⁾ and 2.8 in pp interactions¹⁷⁾.

Long range charge compensation can be particularly well described by the quantity

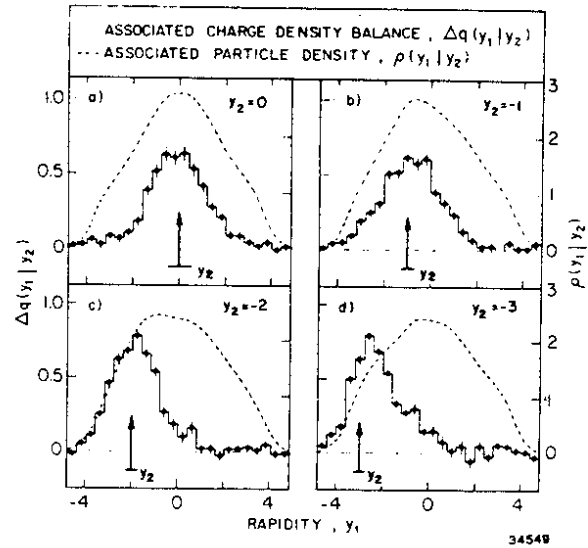


Fig.17 Associated charge density balance [eq.(III.6)] measured by CCHK Collaboration¹⁷⁾ in pp collisions at $\sqrt{s} = 52.5$ GeV.

The curves in Fig. 16 represent the predictions of the fragmentation model MC($q\bar{q} + qq\bar{q}$) mentioned previously. No adjustment of the parameters to any correlation data was done.

$$A(y,y') = \frac{\Phi(y,y')}{\rho_2(y,y')} = \frac{(\rho^{+-} + \rho^{-+}) - (\rho^{++} + \rho^{--})}{(\rho^{+-} + \rho^{-+}) + (\rho^{++} + \rho^{--})}, \quad (\text{III.7})$$

the compensating charge flow per particle pair, which has the structure of an asymmetry. For hypothetical events of charge 0, random charge distribution and constant charged multiplicity n this quantity would be identical to $1/(n - 1)$.

Fig. 18a) to d) shows $A(y,y')$ for e^+e^- annihilation at $\sqrt{S} = 34$ GeV. Whereas for low values of $|y'|$ $A(y,y')$ does not show any pronounced structure apart from a local enhancement at $y \approx y'$, the outermost y' interval $y' < -2.5$ exhibits a very clear separation between short range and long range compensation. Charge compensation is extremely strong for y values near y' , passes a minimum at $y \sim 1$ and rises again as y moves to more positive values in the hemisphere opposite to y' . This second rise is a clear long range effect due to the charge of the primary partons. In fact, assuming the production of two neutral partons, e.g. two gluons that follow Field-Feynman fragmentation, it can be shown that $A(y,y' < -2.5)$ in Fig. 18d) would decrease monotonically with increasing y , being practically 0 for $y > 1$, in disagreement with the data.

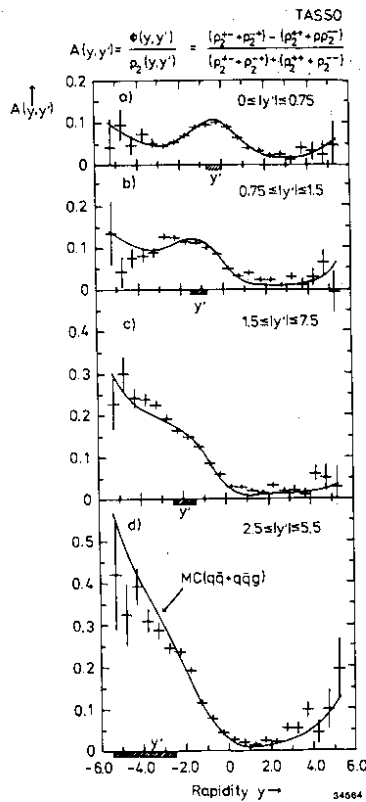


Fig.18 Compensating charge flow per charged hadron pair [eq.(III.7)], measured by TASSO Collaboration³⁾ in $e^+e^- \rightarrow$ hadrons at $\sqrt{S} = 34$ GeV.

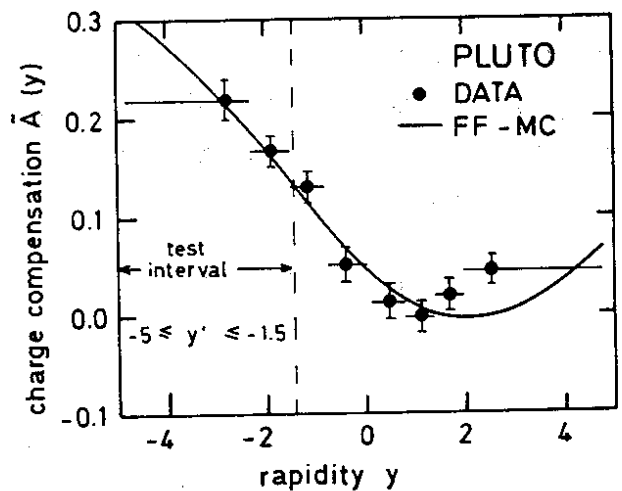


Fig.19 Strength of charge compensation per charged hadron pair, $A(y)$ as a function of y for particles produced in the test interval $-5 \leq y' \leq -1.5$. Measured by PLUTO Collaboration¹⁸⁾ in $e^+e^- \rightarrow$ hadrons at $\sqrt{S} \sim 30$ GeV.

Lower statistics data from the PLUTO Collaboration are shown in Fig. 19. They are in agreement with the TASSO data in Fig. 18d).

If we assume that the charge correlations between the intervals $y' < -2.5$ and $y > 2$, separated from each other by 4.5 units of rapidity, are entirely due to the charge of the primary quarks, we can actually calculate the differential probability $p(y)$, valid in the interval $|y| > 2$, for the assumption that a particle produced in this interval contains the primary quark. Fig. 20 shows a sketch of $\phi(y,y' < -2.5)$ and $A(y,y' < -2.5)$ and as hatched area the regions between which charge compensation is entirely due to the charge of the primary quarks.

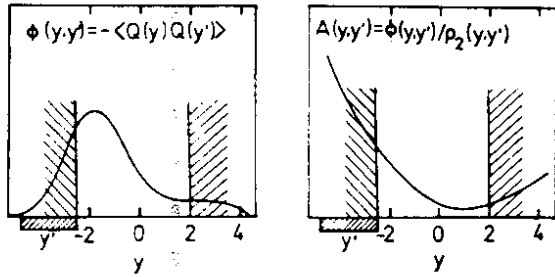


Fig.20 Sketch of the quantities $\phi(y,y')$ [eq.(III.4)] and $A(y,y')$ [eq.(III.7)] for $y' < -2.5$. Charge correlations between the hatched y'/y regions are assumed to be due to the charge of the primary quarks only.

For the average number of pairs that can be formed between the particles produced in the intervals Δy and $\Delta y'$, respectively, we write

$$\begin{aligned} \langle N_{\text{particle pairs}}(y,y') \rangle &= \\ &= \Delta y \Delta y' \rho_2^{cc}(y,y') \left(\frac{3}{2}\right)^2 \end{aligned} \quad (\text{III.8})$$

where ρ_2^{cc} is the two-particle density of charged particles. Assuming half as many neutral as charged particles in the final state, the factor $\left(\frac{3}{2}\right)^2$ in eq.(III.8) converts ρ_2^{cc} into ρ_2^{all} , which includes also neutral particles. For the average number of primary quark pairs in $\Delta y, \Delta y'$ we write

$$\begin{aligned} \langle N_{\text{prim. q pairs}}(y,y') \rangle &= - \Delta y \Delta y' \langle Q(y)Q(y') \rangle / e_{q \text{ eff}}^2 = \\ &= \Delta y \Delta y' \phi(y,y') / e_{q \text{ eff}}^2 \end{aligned} \quad (\text{III.9})$$

where $Q(y)$ is the charge density at y in an event and $e_{q \text{ eff}}^2$ denotes the effective quark charge squared which is defined as averaged over the produced primary quarks $q_p = u,d,s,c,b$ with weights proportional to e_q^2 . Since only quark charge differences can be observed, $e_{q \text{ eff}}^2$ is also averaged over the quarks $q_f = u,d,s$ participating in fragmentation:

$$e_{q \text{ eff}}^2 = \langle (e_{q_p} - \langle e_{q_f} \rangle)^2 \rangle = 0.305 \quad (\text{III.10})$$

if the mean charge of the fragmentation quarks is chosen to be $\frac{1}{15}$ 5).

The product of probabilities that a particle produced at y and another one produced at y' both contain a primary quark (or antiquark) is

$$p(y)p(y') = \frac{\langle N_{\text{prim. q pairs}}(y,y') \rangle}{\langle N_{\text{particle pairs}}(y,y') \rangle} = \quad (III.11)$$

$$= \left[\Phi(y,y')/e_{q \text{ eff}}^2 \right] / \left[\rho_2^{cc}(y,y') \left(\frac{3}{2}\right)^2 \right] = \frac{4}{9} A(y,y')/e_{q \text{ eff}}^2$$

Thus choosing a fixed y' interval ($y' < -2.5$) the quantity $A(y,y')$ in the region $y > 2$ will be proportional to the probability $p(y)$ that a particle at y contains the primary quark. From the measured quantity $\Phi(y,y')$ one calculates with relation (III.11) first the average value $p(|y'| > 2.5) = 0.25$ and with this result the probability $p(|y| > 5) = 0.95 \pm 0.35$, which corresponds to the last data point in Fig. 18d). This high probability value shows that the observed long range correlations in e^+e^- are actually saturated within the framework of the quark model, i.e. the observed effect could hardly be stronger.

It is interesting to consider a similar quantity for the fast particles of the u quark current jet observed in $\nu p \rightarrow \mu^- + \text{hadrons}$. With Feynman x as longitudinal variable we can write

$$p(x) = \langle Q(x) \rangle / \left[\frac{3}{2} \rho^c(x) (e_u - \langle e_{q_f} \rangle) \right] \quad (III.12)$$

where $\langle Q(x) \rangle$ is the charge density, $\rho^c(x)$ the charged particle density and e_u the charge of the u quark.

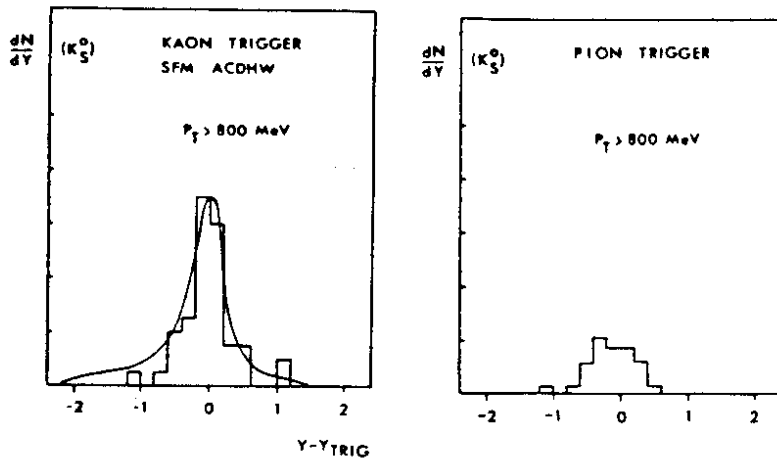
Using the exponential parametrization of the inclusive π^+/π^- production cross section $d\sigma/dx$ in $\nu p \rightarrow \mu^- + \text{anything}$ ¹⁹⁾, we find for $x \rightarrow 1$ the value $p(x \rightarrow 1) = 0.76$, within errors in good agreement with that obtained for e^+e^- at high y .

Conclusions on charge correlations.

- Short range charge compensation in e^+e^- is the same as in pp , with a charge compensation length (FWHM) of 2.8 units in rapidity.
- Long range charge correlations in e^+e^- , attributed to the charge of primary quarks, are well separated from short range effects.
- The fraction of primary quarks contained in high y particles from e^+e^- can be determined by measurements of charge correlations. It is found to be substantial and agrees with that obtained for high x particles in the u quark (current) jet from νp interactions.

IV. Flavour and Baryon Number Correlations.

Unfortunately not many data on correlations of this type are available at present. A first evidence for local conservation of strangeness in phase space was reported from an experiment with the SFM detector investigating



34547

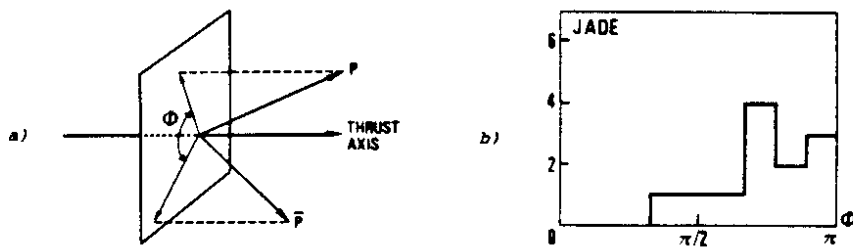
Fig.21 Rapidity y of K^0 's with respect to the rapidity y_{TRIG} of the triggering K^\pm (a) or π^\pm (b), measured in high p_t proton-proton collisions²⁰). ACDHW Collaboration

high p_t reactions at the CERN ISR²⁰). When triggering on a charged kaon with high transverse momentum it was observed that an associated K^0 is produced more often in neighbouring regions of phase-space than if the high p_t trigger was due to a pion.

This is illustrated in Fig.21 where the distribution of $\Delta y = y_{K^0} - y_{TRIG}$ is shown for triggering K^\pm and π^\pm .

A very pronounced peak at $\Delta y \approx 0$ is observed for K^\pm triggers whereas π^\pm triggers yield a much flatter distribution. This has to be taken as clear evidence for local strangeness conservation.

As to baryon-antibaryon correlations, only data from the JADE Colla-



34580

Fig.22 Azimuth angle ϕ formed by the emission directions of a baryon and an antibaryon produced in $e^+e^- \rightarrow$ hadrons, measured by JADE Collaboration²¹).

axis as sketched in Fig. 22a). In the ϕ distribution plotted in Fig. 22b) most of the entries have $\phi > 90^\circ$. This observation suggests local transverse momentum compensation in baryon pair production.

laboration at PETRA are available²¹). It was observed that proton and Δ pairs identified at low momenta ($p \leq 1$ GeV/c) are preferentially emitted in opposite directions of the azimuth angle ϕ , defined with respect to the thrust

V. Bose-Einstein Correlations Between Identical Particles.

In 1960 G. Goldhaber, S. Goldhaber, W. Lee and A. Pais reported²²) on an observation made in $p\bar{p}$ annihilation, that identical pions stick closer together in phase space than pions of different charge. They explained their observation, nowadays often called the GGLP effect, as a consequence of Bose-symmetrization of the multipion wave function. It was realized only later²⁴)

that the effect observed in hadronic reactions was essentially the same as a second order interference phenomenon of photons which was proposed by R.Hanbury Brown and R.Q. Twiss in 1954 and successfully employed afterwards as a method to measure the diameter of discrete radio sources in the universe²³⁾. Whereas in the latter case the interference in the coincidence rate between two detectors ~100 km apart occurs near the detector, in the GGLP case the interference occurs already within or near the particle source.

The GGLP effect, originally observed in $p\bar{p}$ annihilation, was subsequently found to be present in practically all multiparticle data samples investigated for this effect²⁵⁾. The radius of the particle source was determined in such measurements to be of the order of 1 Fermi, as expected.

Last year G. Goldhaber²⁶⁾ presented the results of an analysis performed with 1.3 million events from $e^+e^- \rightarrow J/\psi \rightarrow \text{hadrons}$. In distinction from previous observations in other reactions, here the effect reaches its maximum possible strength, signaling a completely incoherent (chaotic) source. Before discussing these and other results we have to present a few formulae describing the effect.

In Fig. 23 we consider the production of two identical pions with momenta \vec{k}_1 and \vec{k}_2 , arising from two sources A and B with coordi-

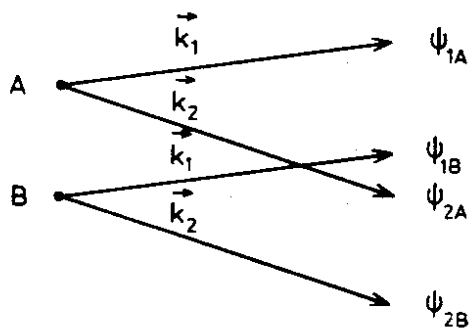


Fig.23 Emission of two identical bosons with momenta \vec{k}_1, \vec{k}_2 from two sources A,B.

if $\pi(\vec{k}_1)$ is emitted from source B and $\pi(\vec{k}_2)$ from source A. In eqs.(V.1, 2) \vec{k} stands for \vec{p}/\hbar and α and β are arbitrary phases of the sources. Since the two pions are assumed to be identical bosons and the observer cannot decide from which source a particular pion was emitted, the coincidence amplitude for simultaneous observation of two pions with momenta \vec{k}_1 and \vec{k}_2 has to be Bose-

nates x_A, x_B . The pion wave functions in the plane wave approximation are

$$\psi_{1A} = e^{-i\vec{k}_1 \vec{x}_A + i\alpha} \quad (V.1)$$

$$\psi_{2B} = e^{-i\vec{k}_2 \vec{x}_B + i\beta}$$

if $\pi(\vec{k}_1)$ is emitted from source A and $\pi(\vec{k}_2)$ from source B. They are

$$\psi_{1B} = e^{-i\vec{k}_1 \vec{x}_B + i\beta} \quad (V.2)$$

$$\psi_{2A} = e^{-i\vec{k}_2 \vec{x}_A + i\alpha}$$

symmetrized:

$$A_{BE} = \psi_{1A} \psi_{2B} + \psi_{1B} \psi_{2A} . \quad (V.3)$$

The corresponding coincidence rate is

$$I_{BE} = |A_{BE}|^2 = 2 + 2 \cos \left[\underbrace{(\vec{k}_1 - \vec{k}_2)}_{\Delta \vec{k}} \cdot \underbrace{(\vec{x}_A - \vec{x}_B)}_{\Delta \vec{x}} \right] \quad (V.4)$$

Note that the arbitrary phases α, β have dropped out from eq.(V.4) which is valid for completely incoherent emission. We define as Bose-Einstein ratio R_{BE} the ratio between I_{BE} and the rate I_0 which would be observed if there were no BE interference:

$$R_{BE} = I_{BE}/I_0 = 1 + \cos [\Delta \vec{k} \cdot \Delta \vec{x}] \quad (V.5)$$

From eq.(V.5) it follows that R_{BE} reaches a maximum value of 2 for $\Delta \vec{k} = 0$. Furthermore it can be seen that the momentum difference $\Delta \vec{k}$ probes the source dimensions in a direction parallel to $\Delta \vec{k}$ ²⁷⁾. More realistic than the binary source considered so far is a source with a Gaussian density distribution of emitting centres: ²²⁾

$$\rho(\vec{r}) \sim \exp\left[-\vec{r}^2/(2 r_0^2)\right] \quad (V.6)$$

which yields as Bose-Einstein ratio

$$R_{BE} = 1 + \exp\left[-r_0^2 \cdot |\vec{k}_1 - \vec{k}_2|^2\right] \quad (V.7)$$

Another parameterization has been suggested by Kopylov and Podgoretskii ²⁸⁾ in the framework of a simple model of a radiating spherical surface of radius R with incoherent pointlike oscillators of lifetime τ :

$$R_{BE} = 1 + \frac{4 J_1^2(q_T R)}{(q_T R)^2} \cdot \frac{1}{1 + (q_0 \tau)^2} , \quad (V.8)$$

where q_T is the transverse component of $\vec{k}_1 - \vec{k}_2$, i.e. $\vec{q}_T \perp \vec{k}_1 + \vec{k}_2$, and $q_0 = E_1 - E_2$. J_1 is the first order Bessel function.

From the symmetrization of the coincidence amplitude of n identical bosons it is straightforward to show that R_{BE} is in the general case equal to $n!$ if all relative momenta $\Delta \vec{k}$ go to zero.

All formulae discussed so far refer to a totally incoherent (chaotic) source which is expected to yield the maximum effect. For partially coherent sources the effect should be smaller and it should be absent in the case of a completely coherent source ^{29,30)}. Therefore the strength of the GGLP

effect is a measure of the incoherence of the source.

In practice the determination of the strength of the effect is more problematic than it may appear at first sight. This is mostly due to the fact that the quantity I_0 in eq.(V.5) to which the effect is normalized, is unphysical. It cannot be measured, but has to be approximated e.g. by using phase space distributions or measured combinations of non-identical particles as reference.

In his analysis of the reaction $e^+e^- \rightarrow J/\psi \rightarrow \text{hadrons}$ G. Goldhaber considers the number ratio R_U^L of equal charge (like) $\pi\pi$ combinations to opposite

charge (unlike) combinations as a function of $Q^2 = M^2 - (2m_\pi)^2$, the squared pion momentum difference in the CM of a pion pair with invariant mass M . An overall normalization factor, the ratio of the numbers of unlike and like $\pi\pi$ combinations in the entire data sample, is employed in the definition of R_U^L , so that pure phase space events would yield $R_U^L \equiv 1$. Fig. 24a) shows R_U^L for pion pairs as a function of Q^2 . An impressive enhancement is observed at $Q^2 \rightarrow 0$. The relative minima at higher Q^2 values are due to K_S^0 and ρ^0 production.

Fig. 24b) shows R_U^L for $K\pi$ combinations. The enhancement as $Q^2 \rightarrow 0$ is considerably reduced, the remaining effect being easily explained as due to misidentified pions.

Cutting out the intervals where K_S^0 and ρ^0 distort the shape a fit of the expression

$$R_U^L = \gamma(1 + \alpha e^{-\beta Q^2}) \quad (V.9)$$

to the data in Fig. 24a) yields $\alpha = 0.71 \pm 0.03$, and $\beta = 18.7 \pm 0.8 \text{ GeV}^{-2}$, which corresponds to a (root mean square) interaction radius of $r = 0.1973 \sqrt{\beta} \text{ GeV Fermi} = 0.85 \pm 0.02 \text{ Fermi}$.

The observed effect can be enhanced when considering only particle pairs with limited values of $\delta = ||p_1| - |p_2||$, a requirement which restricts

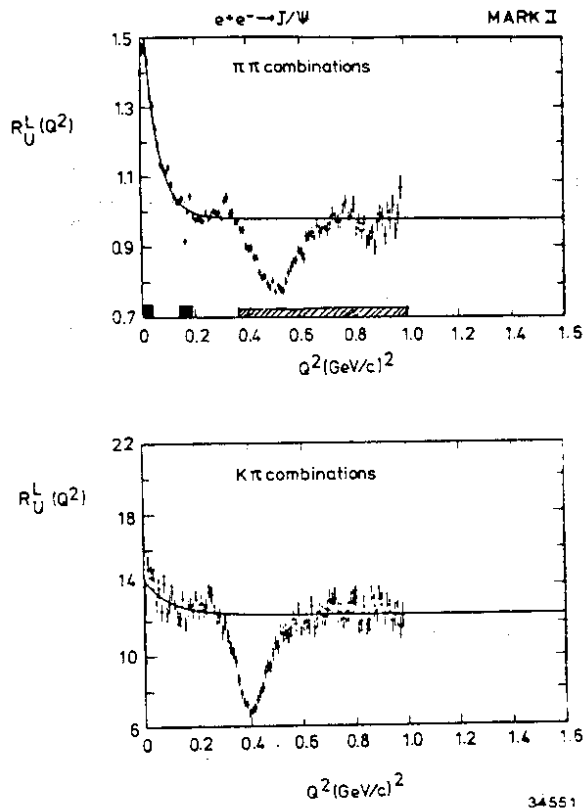


Fig.24 The GGLP effect in $e^+e^- \rightarrow J/\psi \rightarrow \text{hadrons}$:²⁶⁾ a) The ratio R_U^L for $\pi\pi$ combinations as a function of Q^2 . b) The same ratio for $K\pi$ combinations. The curve in a) is a fit of the expression $\gamma[1 + \alpha \exp(-\beta Q^2)]$ to the data yielding $\alpha = 0.71 \pm 0.03$ and $\beta = 18.7 \pm 0.8 \text{ GeV}^{-2}$.

essentially the difference in longitudinal momentum, thus projecting out according to eq.(V.5), the transverse dimensions of the source.

In Fig. 25 the ratio R_U^L is plotted for various values of δ , the enhancement at $Q^2 \rightarrow 0$ being strongest for $\delta < 0.1$ GeV/c yielding $\alpha = 0.94 \pm 0.01$

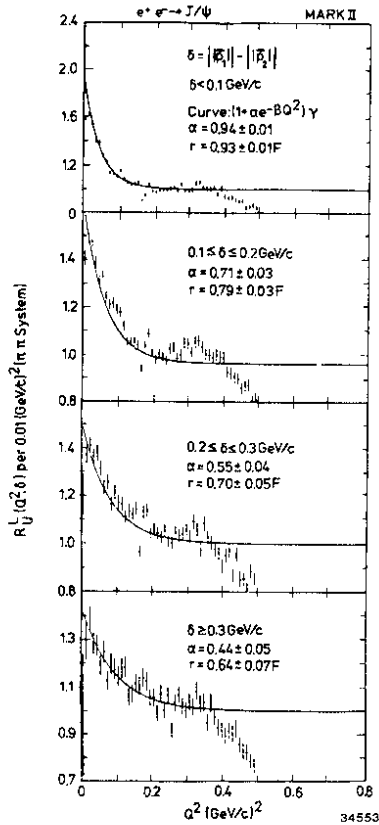


Fig.25 The GGLP effect in $e^+e^- \rightarrow J/\psi \rightarrow \text{hadrons}^{26)}$: The ratio R_U^L for $\pi\pi$ combinations with different values of $\delta = ||\vec{p}_1|| - ||\vec{p}_2||$ as a function of Q^2 25)

eq.(V.9) yields $\alpha_3 = 2.33 \pm 0.06$, $r_3 = 0.49 \pm 0.003$ Fermi. Since the denominator of the ratio contains an enhancement factor due to two identical pions which is $1 + \alpha = 1.89$ at $Q^2 = 0$, the corrected BE ratio, which would be preferentially measured by $R_{\pi^+\pi^-\pi^0}^{\pi^+\pi^+\pi^-}$ ($Q^2 \rightarrow 0$), is obtained by multiplying $R_{\pi^+\pi^+\pi^+}^{\pi^+\pi^+\pi^+}$ by the factor $1 + \alpha = 1.89$ yielding at $Q^2 = 0$ a value of 6.2. Thus the theoretical maximum $n!$ for the n -particle BE ratio at $Q^2 = 0$ is reached, suggesting complete chaoticity of the J/ψ source.

Off resonance e^+e^- data at energies between 4 and 7 GeV $^{26)}$ analysed in the same way show a weaker effect: $\alpha = 0.52 \pm 0.06$, $r = 0.77 \pm 0.08$ Fermi, which might be indicative of a more coherent behaviour of the source in $e^+e^- \rightarrow 2$ jets.

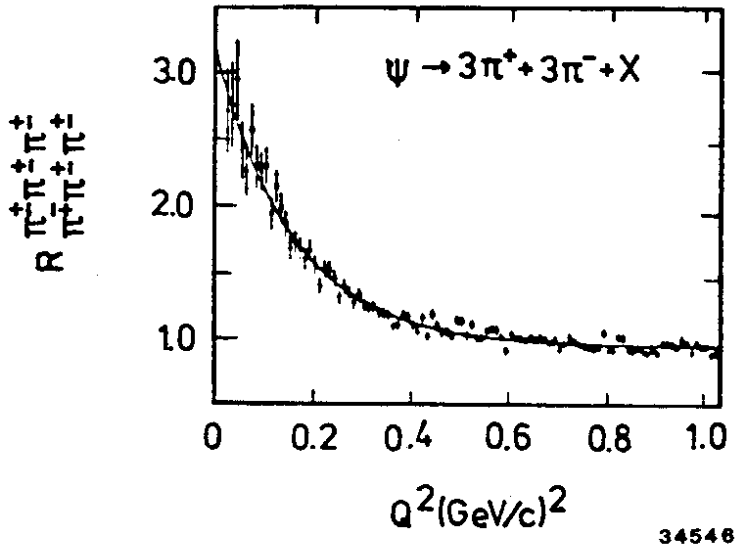


Fig.26 The GGLP effect in $e^+e^- \rightarrow J/\psi \rightarrow \text{hadrons}^{26)}$: Three-pion ratio $R_{\pi^+\pi^+\pi^+}^{\pi^+\pi^+\pi^+}$ as a function of $Q^2(3\pi)$.

The effect is also observed in 3-pion correlations as shown in Fig. 26. Here the ratio $R_{\pi^+\pi^+\pi^+}^{\pi^+\pi^+\pi^+} + \text{c.c.}$, containing a similar overall normalization factor as the ratio R_U^L , is plotted versus $Q^2 = M^2 - (3m_\pi)^2$, where M is in this case the invariant mass of the 3-pion system. A fit to the functional form of

Fig. 27 shows plots of a preliminary analysis from TASSO³⁾ for e^+e^- at 34 GeV. In Fig. 27a) the ratio of the two-particle densities ρ^{++} and ρ^{+-} is displayed as a function of $Q^2 = M^2 - (2m_\pi)^2$. Fig. 27b) shows the corresponding plot for the ratio of 3-particle densities ρ^{+++}/ρ^{++-} with $Q^2 = M^2 - (3m_\pi)^2$. The indices of the densities are a shorthand for all combinations having the same absolute net charge, e.g. $\rho^{++} \rightarrow \rho^{++} + \rho^{--}$ or $\rho^{+-} \rightarrow \rho^{+-} + \rho^{-+}$, their sequence being irrelevant. The ratios do not contain an overall normalization factor.

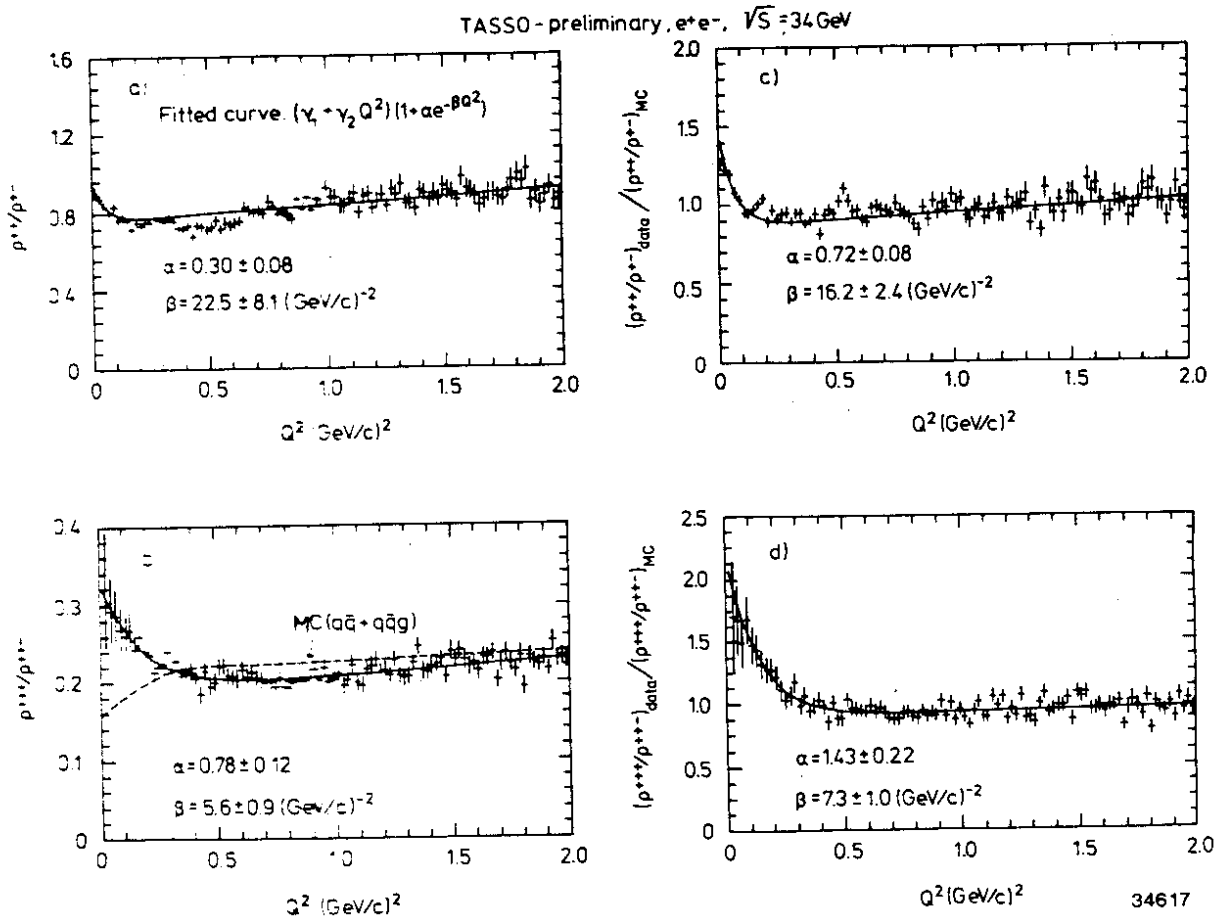


Fig.27 The GGLP effect in $e^+e^- \rightarrow$ hadrons at $\sqrt{S} = 34$ GeV³⁾ Preliminary!
a) 2-pion, b) 3-pion charge ratios as a function of Q^2 . c) 2-pion, d) 3-pion MC-corrected charge ratios as a function of Q^2 .

Both 2-particle and 3-particle ratios exhibit the expected enhancement at $Q^2 = 0$. Fitting the functional form

$$R = (\gamma_1 + \gamma_2 Q^2)(1 + \alpha e^{-\beta Q^2}) \quad (V.10)$$

to the data which allows for a linear background term one obtains for the 2-particle ratios $\alpha = 0.30 \pm 0.08$, $\beta = 22.5 \pm 8.1$ (GeV/c)⁻² and for the 3-particle ratios $\alpha_3 = 0.78 \pm 0.12$, $\beta_3 = 5.6 \pm 0.9$ (GeV/c)⁻². It is questionable,

however, whether this is the correct procedure. This is because the jet fragmentation model which does not contain the GGLP effect, predicts a non-linear drop of the ratios ρ^{++}/ρ^{+-} and ρ^{+++}/ρ^{++-} as Q^2 goes to 0, as a consequence of local charge compensation.

For the 3-particle ratio the prediction of MC($q\bar{q} + q\bar{q}g$) is drawn in Fig. 27b) as dashed line. Since the BE ratio defined in eq.(V.5) compares the physical observation to an (unphysical) theory which takes into account all physics laws except BE symmetrizations, it appears more justified to compare the data to the Monte Carlo prediction rather than to a linear background extrapolation when trying to determine the strength of the effect. It has to be noted that the drop of ρ^{++}/ρ^{+-} and ρ^{+++}/ρ^{++-} predicted by MC($q\bar{q} + q\bar{q}g$) for $Q^2 \rightarrow 0$ is insensitive to the choice of fragmentation parameters.

Normalizing the effect to the MC prediction is easily achieved by fitting the expression of eq.(V.10) to the MC corrected ratios, e.g. $(\rho^{++}/\rho^{+-})_{\text{data}}/(\rho^{++}/\rho^{+-})_{\text{MC}}$. This method avoids problems of absolute normalization. Figs. 27c),d) display the MC corrected ratios for 2- and 3-particle combinations as well as the fitted curves. In all 2-particle fits the Q^2 intervals affected by K^0 and ρ^0 production were eliminated. The results of the fits to the MC corrected data are: $\alpha = 0.72 \pm 0.08$, $\beta = 16.2 \pm 2.4 \text{ (GeV/c)}^{-2}$, $\alpha_3 = 1.43 \pm 0.22$, $\beta_3 = 7.3 \pm 1.0 \text{ (GeV/c)}^{-2}$. The strength of the effect has considerably increased by the MC correction.

In Fig. 28 we show that the GGLP effect is also observed in 4-particle combinations of e^+e^- annihilation events.

The results on the effect observed in e^+e^- annihilation are summarized in Table II. Evidently the GGLP effect is maximally developed on the J/ψ , perhaps a particular feature of the 3-gluon final state, which might act as a more incoherent source than one-chain (= 2-jet) production off resonance³¹⁾. Off resonance the strength of the effect depends, however, on normalization. Normalization to a linear background yields for the TASSO data a substantially smaller effect than normalization to the shape predicted by the jet fragmentation model. In fact with the MC normalization the two-particle combinations from TASSO, although containing the background from $K\pi$ combinations, show an effect as strong as that observed on the J/ψ without cut in δ . When the TASSO data are normalized to a linear background the effect is still stronger than that found by MARK II in e^+e^- at 29 GeV, for which the preliminary values $\alpha = 0.12 \pm 0.12$ and $\alpha_3 = 0.1 \pm 0.1$ have been quoted³²⁾. Note, however, that also the TASSO data are preliminary.

Table II. Recent measurements of the GGLP effect

Experiment	Reaction	\sqrt{s} (GeV)	R _{BE}	δ (+) (GeV/c)	Comments	α (*)	β (*) (GeV ⁻²)	r (Fermi)
Mark II ²⁶⁾	e^+e^-	J/ ψ (3.1)	R ₊₋ ⁺⁺	all δ	-	0.71 ± 0.03	18.7 ± 0.08	0.85 ± 0.02
"	"	"	"	$\delta < 0.1$	-	0.94 ± 0.01	22.2 ± 0.2	0.93 ± 0.01
"	"	"	"	0.1 < $\delta < 0.2$	-	0.71 ± 0.01	16.0 ± 1.2	0.79 ± 0.03
"	"	"	"	0.2 < $\delta < 0.3$	-	0.55 ± 0.04	12.6 ± 1.7	0.70 ± 0.05
"	"	"	"	all δ	J/ $\psi \rightarrow 3\pi^+ + 3\pi^- + X$	0.89 ± 0.03	15.6 ± 0.08	0.78 ± 0.02
TASSO prelim. ³⁾	"	4 - 7	"	all δ	"	0.52 ± 0.06	15.2 ± 3.1	0.77 ± 0.08
"	"	34	"	all δ	-	0.30 ± 0.08	22.5 ± 8.1	0.94 ± 0.17
Mark II ²⁶⁾	"	J/ ψ (3.1)	R ₊₋ ⁺⁺⁺	"	MC normal.	0.72 ± 0.08	16.2 ± 2.4	0.79 ± 0.06
TASSO prelim. ³⁾	"	34	"	"	J/ $\psi \rightarrow 3\pi^+ + 3\pi^- + X$	2.33 ± 0.06	6.2 ± 0.1	0.49 ± 0.003
"	"	"	"	"	-	0.78 ± 0.12	5.6 ± 0.9	0.47 ± 0.04
Bubbl ch. ³³⁾	π^+p	5.6	R ₊₋ ⁺⁺	"	MC normal.	1.43 ± 0.22	7.3 ± 1.0	0.53 ± 0.04
"	"	"	R ₊₋ ⁺⁺	"	+)	0.49 ± 0.02	-	1.84 ± 0.06
"	"	"	R ₊₋ ^{++resh.}	"	+)	0.88 ± 0.02	-	1.45 ± 0.04
"	"	"	R ₊₋ ^{++resh.}	"	+)	0.76 ± 0.02	-	1.43 ± 0.05

*) α, β defined by eq. (V. 9)

+) $\delta = || p_1 | - | p_2 ||$

+) Fit to eq. (V.8) with factor α in front of interference term. Note that r has a different meaning here than in the fits to e^+e^- data. See eq. (V. 8)

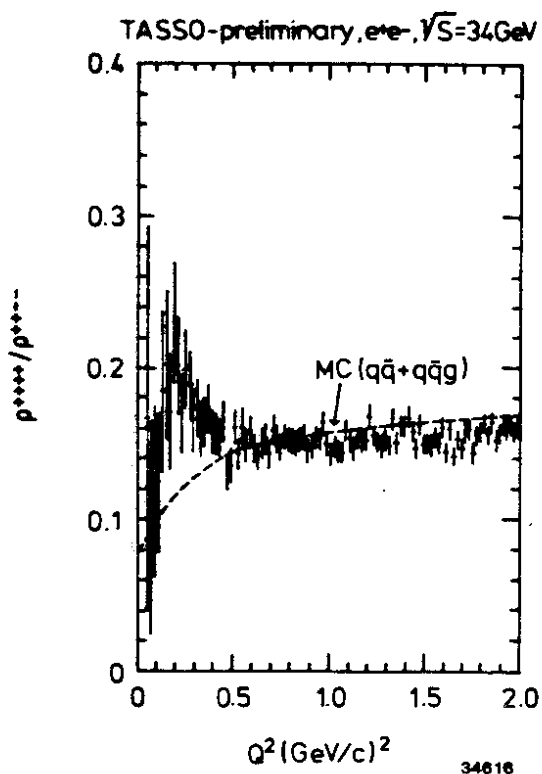


Fig.28 The GGLP effect in 4π combinations as a function of Q^2 (4π) in $e^+e^- \rightarrow \text{hadrons}$ at $\sqrt{S}=34$ GeV ³⁵⁾. Preliminary!

In a recent preprint of a bubble chamber collaboration ³²⁾ the GGLP effect is investigated in two-pion combinations of 16 GeV/c π^+p and K^-p interactions and in $p\bar{p}$ annihilations at rest. The effect is studied with different normalization procedures. Besides the usual normalization to $\pi^+\pi^-$ combinations denoted by the ratio $R_{BE} = R_{+-}^{++}$ the authors also used for the denominator in R_{BE} pion combinations where transverse momenta had been "reshuffled", i.e. interchanged at random in a given event. This leads to the ratios $R_{BE} = R_{(+)-}^{++}$ and $R_{(++)}^{++}$. The ratios were analyzed using eq.(V.8) where the Bessel function term was multiplied by the free parameter α . The fitted values of α and r are quoted in Table II for π^+p interactions. The data from K^-p and $p\bar{p}$ interactions yield similar results. We

observe that the strength of the effect is considerably increased when normalizing the Bose-Einstein ratio to reshuffled pion pairs. The larger values of the source radius in comparison to the e^+e^- results are due to the different functional form (eq. V.8) employed in the fit: here the radius refers to an emitting spherical surface, whereas for e^+e^- r was assumed to be the root mean square radius of a spatial Gaussian distribution.

On the basis of the topological expansion approach Giovannini and Veneziano ³¹⁾ predict a scaling law for the strength of the Bose-Einstein enhancement in reactions involving different numbers of chains. It reads

$$\alpha = R_{BE}(Q^2 = 0) - 1 = 1 - \text{const}/n_{\text{chain}} \quad (\text{V.11})$$

Using the value $\alpha = 0.5 \pm 0.1$ found for pp collisions ³⁴⁾ (involving two chains) they predict with eq.(V.11) for e^+e^- annihilation (one chain) a value of $\alpha = 0.0 \pm 0.2$. Given the experimental errors and normalization uncertainties, such a prediction cannot be ruled out yet. However problems may arise for relation eq.(V.11) if one takes as granted that α is equal to 1 in J/ψ decays. This would imply $\text{const} = 0$ and therefore the maximum Bose-Einstein effect for all reactions.

Conclusions on Bose-Einstein Correlations.

- The GGLP effect reaches maximum strength in the reaction $J/\psi \rightarrow$ hadrons, signaling a completely chaotic source.
- In e^+e^- annihilation the effect seems to decrease with increasing energy. Definitive statements are difficult due to systematic uncertainties caused by normalization problems.
- In order to come to more reliable determinations of the quantities describing Bose Einstein correlations, deeper theoretical and experimental understanding of all the problems involved is needed. In particular sufficient clarification of the concept of coherence and chaoticity of a source in particle physics would be highly desirable.

ACKNOWLEDGEMENTS

The author appreciates very valuable discussions with Susan Cooper, Henryk Kowalski, Peter Mättig, Wolfgang Ochs, Paul Söding, Günter Wolf and Andrzej Wróblewski.

REFERENCES

- 1) G. Giacomelli and M.Jacob, "Physics at the CERN-ISR", Physics Reports Vol. 55/1 (1979).
- 2) ABCHW Collaboration, A.Breakstone et al., Phys.Lett. 114B (1982) 383.
- 3) Private communication from TASSO Collaboration.
- 4) D.Fournier, Proceedings of the 1981 International Symposium on Lepton and Photon Interactions at High Energies, p.102; published by Universität Bonn, Physikalisches Institut.
- 5) R.D.Field and R.P.Feynman, Nucl.Phys. B136 (1978) 1.
- 6) P.Hoyer et al., Nucl.Phys. B161 (1979) 349
- 7) TASSO Collaboration, R.Brandelik et al., Phys.Lett. 94B (1980) 437.
- 8) TASSO Collaboration, R.Brandelik et al., DESY report 82-046, accepted for publication in Phys.Lett.
- 9) G.Veneziano, Nucl.Phys. B117 (1976) 519;
A.Capella, U.Sukhatme and J.Tran Thanh Van, Z.Physik C, Particles and Fields 3 (1980) 329;
For a recent review see A.Capella, Proc. Europhysics Study Conf., Erice, 1981, ed. R.T. Van de Walle.
- 10) A.Wróblewski, Talk presented at DESY, August 31, 1981 and private communication.

- 11) J.Gaudean, "Latest results from the UA5 Collaboration", invited paper to this conference.
- 12) J.H.Kühn and H.Schneider, Zeitschr. f. Physik C8 (1981) 115.
- 13) J.Benecke et al., Phys.Lett. B57 (1975) 447;
J.Benecke and H.Kühn, Nucl.Phys. B740 (1978) 179.
- 14) K.Fiałkowski and A.Kotański, preprint MPI-PAE/PTh 7/82. also paper 64/C2 contributed to this conference.
- 15) N.Schmitz, Rapporteur's Talk, Proceedings of the 1981 International Symposium on Lepton and Photon Interactions at High Energies, p.534; published by Universität Bonn, Physikalisches Institut.
- 16) TASSO Collaboration, R.Brandelik et al., Phys.Lett. 100B (1981) 357.
- 17) CERN-Collège de France-Heidelberg-Karlsruhe Collaboration, D.Drijard et al., Nucl.Phys. B166 (1980) 233.
- 18) PLUTO Collaboration, Ch.Berger et al., DESY report 82-058, to be published.
- 19) N.Schmitz, Proceedings of the XII. International Symposium on Multi-particle Dynamics. Notre Dame 1981, p.492; also Report MPI-PAE/Exp.E1.93.
- 20) H.G.Fischer, Rapporteur's Talk, Proceedings of the International Conference on High Energy Physics, Lisbon 1981.
- 21) JADE Collaboration, W.Bartel et al., Phys.Lett. 104B (1981) 325.
- 22) G.Goldhaber, S.Goldhaber, W.Lee and A.Pais, Phys.Rev. 120 (1960) 300.
- 23) R.Hanbury Brown and R.Q. Twiss, Phil.Mag. 45 (1954) 663; Nature 178 (1956) 1046;
E.M.Purcell, Nature 178 (1956) 1449.
- 24) V.G.Grishin, G.I.Kopylov and M.I.Podgoretskii, Soviet Nuclear Phys. 13 (1970) 1116.
E.V.Shuryak, Phys.Lett. 44B(1973) 387.
- 25) M.Deutschmann et al., CERN Report CERN/EP/PHYS 78-1 (1978).
- 26) G.Goldhaber "Multipion Correlations in e^+e^- Annihilation at SPEAR", presented at the International Conference on High Energy Physics, Lisbon, 1981; also Report LBL-13291.
- 27) G.Cocconi, Phys.Lett. 49B (1974) 459.
- 28) G.I.Kopylov and M.I.Podgoretskii, Soviet Nuclear Phys. 18 (1973) 656;
G.I.Kopylov, Phys.Lett. 50B (1974) 472.
- 29) G.N.Fowler and R.M.Weiner, Phys.Lett. 70B (1977) 201.
- 30) M.Gyulassy, S.M.Kauffmann and Lance W.Wilson, Phys.Rev. C20 (1979) 2267.
- 31) A.Giovannini and G.Veneziano, Nucl.Phys. B130 (1977) 61.
- 32) G.Goldhaber, Branff Summer School 1981, preliminary.
- 33) M.Deutschmann et al., CERN/EP 82-43, submitted to Nucl.Phys. B.
- 34) E.L.Berger et al., Phys.Rev. D15 (1977) 206.